doi.org/10.36721/PJPS.2026.39.9.265.1

Effect of quercetin on aconitine-induced renal interstitial fibrosis and its relationship with PI3K/Akt pathway

Wei Feng[1], Jie Zhou[2], Yuanjue Zheng[3] and Yingang Li[4]*

[1]Department of Nephrology, The 927th Hospital of the Joint Support Force of the People's Liberation Army of China, Pu'er, Yunnan, 665000, China

[2]Department of Urology, The 927th Hospital of the Joint Support Force of the People's Liberation Army of China, Pu'er, Yunnan, 665000, China

[3]Department of Gastroenterology, The 927th Hospital of the Joint Support Force of the People's Liberation Army of China, Pu'er, Yunnan, 665000, China

[4]Department of Dentistry, The 927th Hospital of the Joint Support Force of the People's Liberation Army of China, Pu'er, Yunnan, 665000, China

Abstract: **Background**: Renal interstitial fibrosis (RIF) is a critical pathological outcome of chronic kidney disease (CKD). Aconitine has been shown to induce RIF, with the phosphatidylinositol 3-kinase/protein kinase B (PI3K/Akt) signaling pathway potentially playing a key role in this process. Quercetin, a natural flavonoid compound, exhibits anti-fibrotic effects that may be associated with this pathway. However, there is no clear evidence yet regarding its role in aconitine-induced RIF. **Objectives**: This study aimed to investigate the intervention effect of quercetin on aconitine-induced RIF and the role of PI3K/Akt pathway in its mechanism. **Methods**: A mouse model of RIF was established and the animals were randomly assigned to the following groups: normal control, aconitine model, low-dose quercetin, medium-dose quercetin, high-dose quercetin and high-dose quercetin combined with the PI3K inhibitor S27673-MA. The extent of fibrosis and the expression of key molecules in the PI3K/Akt pathway were evaluated using histopathology, qPCR and Western blot. **Results**: Compared to the model group, the high-dose quercetin group exhibited an approximately 60% reduction in fibrotic area ($P<0.01$). Moreover, quercetin significantly suppressed the overexpression of phospho-PI3K (p-PI3K), phospho-AKT (p-AKT), neutrophil elastase (NE) and nuclear factor kappa B p65 (NF-κB p65) at both transcriptional and protein levels in renal tissues ($P<0.05$). The use of the PI3K inhibitor S27673-MA further enhanced the anti-fibrotic effect of quercetin and its inhibitory effect on the aforementioned molecules. **Conclusion**: Quercetin ameliorates aconitine-induced RIF by inhibiting the PI3K/Akt pathway and its downstream NE/NF-κB axis.

Keywords: Aconitine-induced RIF; PI3K/Akt; Quercetin

Submitted on 02-12-2025 – Revised on 02-02-2026 – Accepted on 09-02-2026

INTRODUCTION

Renal interstitial fibrosis (RIF) is the common pathological outcome of various chronic kidney diseases progressing to end-stage renal disease. It is characterized by tubular atrophy, capillary loss, inflammatory cell infiltration and excessive deposition of extracellular matrix, ultimately leading to irreversible loss of renal function. Exploring effective strategies to intervene in renal interstitial fibrosis is of great significance for delaying the progression of chronic kidney disease.

As a diester-type diterpenoid alkaloid with confirmed nephrotoxicity, aconitine is commonly used as a tool compound for studying drug-induced kidney injury and secondary fibrosis. Its toxic mechanisms are closely related to the induction of oxidative stress and activation of inflammatory responses. Aconitine promotes the massive generation of reactive oxygen species in renal tissues and activates key inflammatory transcription factors such as nuclear factor-κB, thereby initiating a series of pro-fibrotic signals (Xiang *et al*., 2023, Rui *et al*., 2024). However, whether and how aconitine nephrotoxicity directly drives the fibrosis process by regulating specific intracellular signaling pathways remains incompletely elucidated.

The phosphatidylinositol 3-kinase/protein kinase B (PI3K/Akt) signaling pathway plays a central role in cell survival, proliferation, metabolism and stress responses. Recent studies have shown that the abnormal and sustained activation of the phosphatidylinositol 3-kinase/protein kinase B (PI3K/Akt) pathway is a key promoter of fibrosis in multiple organs (e.g., cardiac, pulmonary and hepatic fibrosis) (Hao *et al*., 2023; Wang *et al*., 2024). Upon activation, this pathway can not only directly upregulate the expression of the pro-fibrotic factor TGF-β but also amplify inflammatory and fibrotic responses by regulating downstream effector molecules such as neutrophil elastase and NF-κB (Xu *et al*., 2020). In the field of kidney research, evidence also suggests that the PI3K/Akt pathway is involved in the regulation of renal fibrosis (Yu *et al*., 2025; Hu *et al*., 2022). This study therefore hypothesizes that aconitine may activate the PI3K/Akt pathway, serving as

**Corresponding author:* e-mail: xfqht89917veco@126.com

an important mechanistic link in its induction of renal interstitial fibrosis.

Quercetin, a natural flavonoid compound, has attracted considerable interest owing to its potent antioxidant, anti-inflammatory and anti-fibrotic properties. Studies have shown that quercetin effectively inhibits the excessive activation of the PI3K/Akt pathway in models of pulmonary and hepatic fibrosis, thereby alleviating fibrotic lesions (He *et al*., 2025; Zhang *et al*., 2025). In terms of renal protection, quercetin has been confirmed to ameliorate acute kidney injury and subsequent fibrosis induced by various factors, with mechanisms involving the reduction of oxidative stress and modulation of autophagy (Zeng *et al*., 2023; Liu *et al*., 2020). These findings suggest that quercetin may be a potential candidate drug for intervening in PI3K/Akt pathway-associated renal fibrosis. However, direct evidence is currently lacking on whether quercetin can specifically counteract aconitine-induced renal interstitial fibrosis by regulating this pathway.

Based on the aforementioned evidence and existing knowledge gaps, we hypothesize that quercetin can alleviate oxidative stress and inflammatory responses induced by aconitine, thereby exerting anti-renal interstitial fibrosis effects by inhibiting the PI3K/Akt signaling pathway and its downstream NE/NF-κB axis. To test this hypothesis, this study will establish a mouse model of renal interstitial fibrosis induced by aconitine, evaluate the interventional effects of different doses of quercetin and comprehensively utilize molecular biology techniques to detect the expression changes of key proteins in the PI3K/Akt pathway and downstream fibrosis-related molecules. The aim is to clarify the pharmacodynamic characteristics and potential molecular mechanisms underlying the renal protective effects of quercetin, providing new experimental evidence for the clinical prevention and treatment of drug-induced kidney injury and renal fibrosis.

MATERIALS AND METHODS

Experimental materials

Main reagents

Quercetin (purity ≥98%, Shanghai Yuanye Bio-Technology Co., Ltd., Batch No.: B20527-20mg). Its dosage selection (50, 100, 150 mg/kg) was based on previous studies demonstrating efficacy and dose-dependency in renal fibrosis models (Liu *et al*., 2019).

Aconitine (purity ≥98%, Shanghai Xuanya Bio-Technology Co., Ltd., Batch No.: 2752-64-9). The administered dose was 1.0 mg/kg, referring to literature establishing subacute kidney injury models (Yangzom *et al*., 2022).

PI3K inhibitor S27673-MA [MCE (China) Haoyuan Biotech, purity ≥ 99.91%, Batch No.: 5142-23-4] and PI3K agonist 740Y-PDGFR [MCE (China) Haoyuan Biotech, purity ≥ 99.67%, Batch No.: 1236188-16-1].

Rabbit anti-phospho-AKT (Ser473) antibody (Cat. No.: ybP001, purity ≥ 99.99%; Shanghai Yuchun Biotechnology, China), Rabbit anti-p-PI3K antibody (Rabbit Anti-Centaurin gamma 1 antibody, purity ≥ 98.00%, Batch No.: K12103-SAR, Beijing Biosynthesis Biotechnology), Rabbit anti-mouse NF-κB p65 polyclonal antibody (purity ≥ 95%, Cat. No.: 10745-1-AP, Proteintech Group, USA), Rabbit anti-mouse Neutrophil Elastase (NE) polyclonal antibody (Cat. No.: bs-20641R, Beijing Biosynthesis Biotechnology Co., Ltd.), Mouse anti-GAPDH monoclonal antibody (Cat. No.: 60004-1-Ig, purity ≥ 95%, Proteintech Group, USA). HRP-labeled goat anti-rabbit secondary antibody was purchased from XINBOSHENG Biotechnology (ab6721).

Main instruments

Automated sample cryogenic grinding instrument (Shanghai Jingxin); iBright™ MCL1000 Imaging system (Invitrogen, Singapore); Quantitative fluorescence PCR instrument (Bio-Rad); vertical electrophoresis and transfer system (Bio-Rad).

Experimental animals

Seventy-two 8-week-old male C57BL/6 mice (SPF grade), weighing 20–22 g, were purchased from Shanghai Senxingyan Biotechnology Co., Ltd. The animals were housed in an SPF environment with constant temperature (22 ± 2)ºC, constant humidity (50 ± 10)% and a 12-hour light/12-hour dark cycle, with free access to food and water. They were acclimatized for one week.

Experimental methods

Animal grouping and model establishment

Mice were randomly divided into 6 groups using a random number table, with 12 mice in each group. Normal Control Group (NC Group): Received intraperitoneal injection of an equivalent volume of normal saline. Model Group: Received intraperitoneal injection of aconitine (1.0 mg/kg) on days 0, 7 and 21. Quercetin Low, Medium and High Dose Groups: Following the same aconitine modeling protocol, these groups received daily oral gavage of quercetin at doses of 50, 100 and 150 mg/kg, respectively, for a continuous intervention period of 14 days. Quercetin High Dose + PI3K Inhibitor Group: Concurrent with the high dose of quercetin, this group received intraperitoneal injection of the PI3K inhibitor S27673-MA (10 mg/kg, three times per week).

The aconitine model was established based on and optimized from previous literature (Yangzom *et al*., 2022). With the exception of the normal control group, mice in all other groups received three intraperitoneal injections of aconitine (1.0 mg/kg) on days 0, 7 and 21 to establish a

stable subacute progressive renal interstitial fibrosis model. Aconitine solutions were prepared immediately before use and all operations were performed under light-protected conditions. A successful model should exhibit vacuolar degeneration and detachment of renal tubular epithelial cells, cast formation, interstitial congestion, hemorrhage and inflammatory cell infiltration.

Sample size calculation: Based on preliminary experimental data, with α=0.05 and test power (1-β)=0.8, calculation using G*Power 3.1 software indicated a minimum requirement of 10 animals per group. To account for potential attrition, each group was set at n=12.

Tissue specimen collection

Twenty-four hours after the last administration, mice were anesthetized. Blood was collected and then the mice were euthanized. Both kidneys were rapidly harvested. One portion was fixed in 4% paraformaldehyde for pathological analysis, while the other portion was flash-frozen in liquid nitrogen and stored at -80°C for subsequent molecular biological assays.

Histopathological analysis

Fixed kidney tissues were dehydrated and cleared through a standard protocol, then embedded in paraffin. Tissue blocks were serially sectioned into 3 μm-thick slices using a paraffin microtome (Leica RM2235). The sections were mounted onto poly-lysine-coated glass slides and baked in a 60℃ oven for 2 hours prior to staining.

Hematoxylin-eosin (HE) staining: After dewaxing in xylene and rehydration through a graded ethanol series, sections were stained with Harris's Hematoxylin for 5 minutes, followed by rinsing with tap water for bluing. Subsequently, sections were counterstained with 0.5% Eosin Y (aqueous solution) for 1 minute. The stained sections were dehydrated through a graded ethanol series, cleared in xylene and finally mounted with neutral balsam. This staining aimed to observe the basic morphological structure of glomeruli and tubules, inflammatory cell infiltration, interstitial congestion and other fundamental pathological changes.

Masson's trichrome staining: A Masson's trichrome staining kit (purchased from Beijing Solarbio Science and Technology Co., Ltd., Cat. No.: G1340) was used to assess collagen fiber deposition in the renal interstitium. After dewaxing and rehydration, sections were processed according to the kit instructions. Key steps were as follows: nuclei were stained with Weigert's iron hematoxylin for 8 minutes and then with Ponceau acid fuchsin solution for 8 minutes. Differentiation was performed with 1% phosphomolybdic acid solution for 2 minutes and finally, collagen fibers were stained with 2% aniline blue solution for 3 minutes. Upon completion, sections were rapidly dehydrated, cleared and mounted. Under a light microscope (Olympus BX53), Masson staining results showed nuclei in black-blue, cytoplasm and muscle fibers in red and collagen fibers in bright blue.

All stained sections were systematically and randomly sampled and photographed by a pathologist blinded to the experimental groups, using a microscope equipped with a digital camera (Olympus DP27). For each kidney tissue section, 10 non-overlapping, complete fields of view containing glomeruli and tubules were randomly selected from the renal cortex region. The Masson-stained images were quantitatively analyzed using professional image analysis software Image-Pro Plus 6.0 (Media Cybernetics, USA). Using the software's color recognition function, a uniform threshold for blue color (collagen fibers) was set to calculate the percentage of blue collagen area relative to the total tissue area (excluding blank areas and lumens) for each field of view. Finally, the average value from the 10 fields of view per animal was taken as the percentage of renal interstitial fibrotic area (Fibrotic Area %) for that sample, for subsequent statistical comparison.

RNA extraction and real-time fluorescence quantitative PCR

Total RNA was extracted from renal tissue using the TRIzol method and reverse-transcribed into cDNA. Using GAPDH as the internal reference gene, qPCR was performed on a QuantStudio 5 system employing the SYBR Green method. Primer sequences are listed in Table 1 and all primers were verified for specificity using BLAST. The relative expression levels of target genes (p-PI3K, p-AKT, NE, NF-κB p65) were calculated using the $2^{-\Delta\Delta Ct}$ method. Three technical replicates were performed for each sample.

Protein extraction and Western blot

Approximately 50 mg of renal tissue was homogenized on ice in RIPA lysis buffer containing protease and phosphatase inhibitors. Protein concentration was determined using the BCA method. Equal amounts of protein (30 μg) were separated by 10% SDS-PAGE electrophoresis and transferred onto PVDF membranes. Membranes were blocked with 5% skim milk at room temperature for 1 hour, followed by overnight incubation at 4°C with primary antibodies (p-PI3K, p-AKT, NF-κB p65, NE, GAPDH; all diluted at 1:1000). After washing with TBST, membranes were incubated with HRP-conjugated secondary antibody (1:5000) at room temperature for 1 hour. Signal detection was performed using ECL ultra-sensitive luminescent solution and images were captured using the iBright system. ImageJ software was used to analyze the grayscale values of target bands. Semi-quantitative analysis was performed using the ratio of the grayscale value of the target protein to that of the internal reference GAPDH.

Statistical analysis

All data are expressed as mean ± standard deviation. Statistical analysis was performed using GraphPad Prism

9.0 software. First, the Shapiro-Wilk test was employed to assess data normality. For multi-group comparisons where data were normally distributed with homogeneity of variance, one-way analysis of variance (ANOVA) was used, followed by Tukey's post hoc test for multiple comparisons. If the assumptions for parametric tests were not met, the Kruskal-Wallis non-parametric test was applied, followed by Dunn's multiple comparisons. A P-value < 0.05 was considered statistically significant.

RESULTS

Mouse model was successfully constructed

Twenty-one days post-injection, mice in the model group exhibited apparent eyelid edema, decreased tail temperature, darkened skin around the mouth, nose, tail and limbs and prominent neurological signs including tremors (head, neck and limbs), ataxia, disoriented movements and intermittent restlessness. At the same time, some glomeruli in the kidney were swollen or pyknotic, the lumen epithelium of the distal convoluted tubules and proximal tubules of the renal tubules was shed and there was exudation and interstitial congestion and bleeding were obvious (Fig. 1A). Masson staining (Fig. 1B) further demonstrated that obvious blue collagen fiber deposition occurred in the renal interstitium of the model group. Quantitative analysis indicated that the percentage of renal interstitial fibrosis area in the model group was 28.5 ± 4.2%, significantly higher than that in the NC group 2.1 ± 0.5% P < 0.001. These results confirmed the successful construction of the renal interstitial fibrosis model.

Quercetin attenuated aconitine-induced RIF in a dose-dependent manner

To assess quercetin's effect on aconitine-induced RIF, through animal experiments, different doses of quercetin were perfused into model mice. The histopathological analysis revealed (Fig. 2A) that, compared to the model group, the quercetin intervention groups showed alleviated renal tubular injury and reduced interstitial collagen deposition, with the improvement effect strengthening as the dose increased. Quantitative analysis of Masson staining (Fig. 2B) indicated that the percentage of renal interstitial fibrotic area in the low-, medium- and high-dose quercetin groups decreased to (21.3 ± 3.5)%, (16.8 ± 2.9)% and (11.4 ± 2.1)%, respectively (all P < 0.01 compared to the model group), demonstrating a clear dose-dependent ameliorative effect (the fibrotic area in the high-dose group was reduced by approximately 60% compared to the model group).

Analysis of immune cell infiltration (Table 2) showed that the numbers of pro-fibrotic $CD68^+$ macrophages and $F4/80^+$ macrophages in the renal interstitium of the model group were significantly increased 18.68±2.34% and 15.32±2.14%, respectively. Quercetin intervention significantly reduced the numbers of both cell types, with the most pronounced effect observed in the high-dose group, decreasing to 7.65±1.17% and 6.87±1.05%, respectively; P < 0.01 compared to the model group.

Molecular-level detection results further supported the above findings. qPCR analysis (Figs. 2C-F) showed that, compared to the NC group, the mRNA expression levels of p-PI3K, p-AKT, NE and NF-κB p65 in the renal tissue of the model group were significantly upregulated (all P < 0.05). After quercetin intervention, the expression levels of these genes decreased in a dose-dependent manner. In the high-dose quercetin group, the mRNA levels of p-PI3K and p-AKT decreased to approximately 45% and 50% of those in the model group, respectively (both P < 0.05), while the expression of NE and NF-κB p65 was also inhibited by approximately 55% and 60%, respectively (both P < 0.05).

Effect of PI3K/Akt pathway on RIF

To directly verify the role of the PI3K/Akt pathway in RIF, this study utilized a pathway agonist (740Y-PDGFR) and an inhibitor (S27673-MA). As shown in fig. 3A, compared to the model group, treatment with the PI3K inhibitor S27673-MA alone significantly reduced renal interstitial collagen deposition, with the fibrotic area decreasing to 15.7 ± 3.0% (P < 0.01 vs. model group). Conversely, treatment with the PI3K agonist 740Y-PDGFR exacerbated fibrosis, increasing the area to 35.2 ± 4.8% (P < 0.05 vs. model group). Analysis of the molecular mechanisms (Figs. 3B-E) revealed that S27673-MA treatment significantly suppressed the expression of p-PI3K, p-AKT, NE and NF-κB p65 at both the gene and protein levels in the renal tissue of model mice (decreases ranging between 40%-65% compared to the model group, all P < 0.01). In contrast, 740Y-PDGFR treatment further enhanced the expression of these molecules (increases of approximately 20%-35%, P < 0.05). Western blot results (Fig. 3F) were consistent with the gene expression trends. These results clearly demonstrate that inhibiting the PI3K/Akt pathway can effectively ameliorate RIF and the mechanism involves the suppression of the downstream NE/NF-κB axis.

Quercetin alleviates aconitine-induced RIF through PI3K/Akt pathway

To investigate whether quercetin exerts its effects through this pathway, this study combined high-dose quercetin with the PI3K inhibitor S27673-MA. Histopathology (Fig. 4A) revealed that the high-dose quercetin plus S27673-MA group exhibited essentially normal renal tubular structure, with almost no inflammatory cell infiltration or epithelial cell swelling. Gene and protein expression analyses revealed a synergistic inhibitory effect. The combined intervention showed stronger inhibition of p-PI3K, p-AKT, NE and NF-κB p65 compared to high-dose quercetin or S27673-MA alone. At the gene level (Figs. 4B-E), the expression of p-AKT and NF-κB p65 in the combination group was inhibited by approximately 75% and 80%, respectively, relative to the model group.

Table 1: Real-time PCR primers and primer sequences.

Primer		Sequences
p-AKT	Forward primer	5'-TGTCTCGTGAGCGCGTGTTTT-3'
	Reverse primer	5'-CCGTTATCTTGATGTGCCCGTC-3'
p-PI3K	Forward primer	5'-CTTGCCTCCATTCACCACCTCT-3'
	Reverse primer	5'-GCCTCTAATCTTCTCCCTCTCCTTC-3'
NE	Forward primer	5'-GGGTCACCATCCAGGAACTCA-3'
	Reverse primer	5'-CACCATCCTGGCGAGTTTCA-3'
NF-kB p65	Forward primer	5'-CAGATACCACTAAGACGCACCC-3'
	Reverse primer	5'-CTCCAGGTCTCGCTTCTTCACA-3'
GAPDH	Forward primer	5'-ATTACCCGCCCGACAATAGG-3'
	Reverse primer	5'-CATGAGTCAGCTAGGCTAGAA-3'

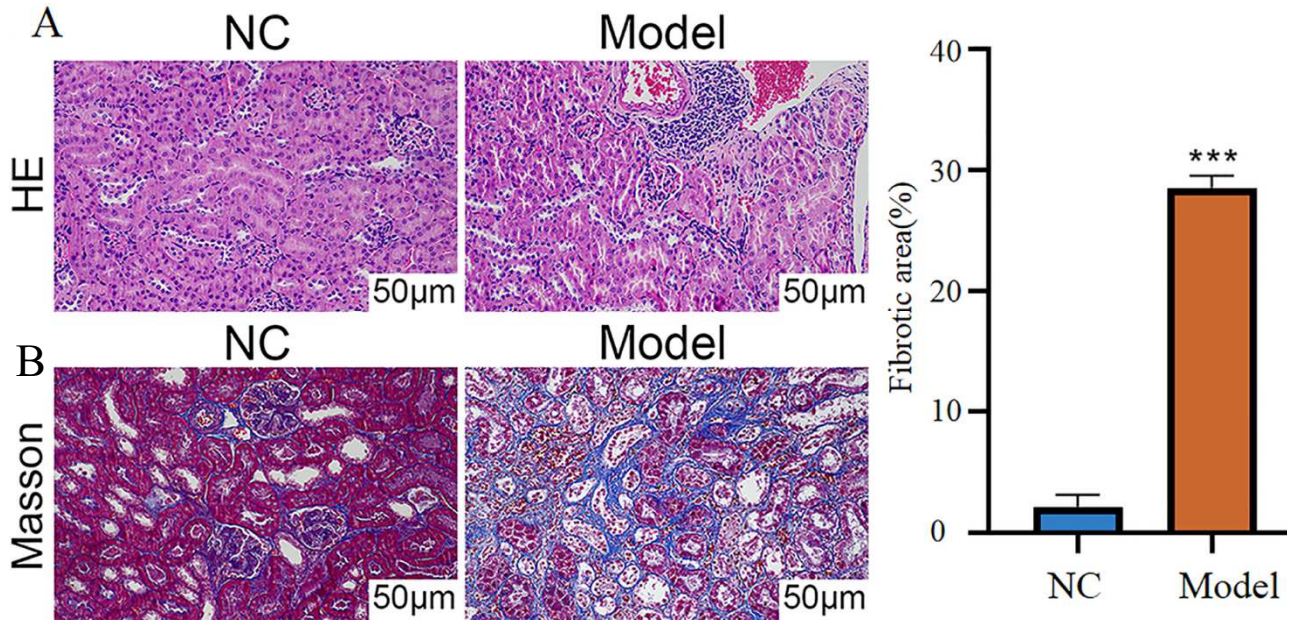

Fig. 1: Successful establishment of the mouse model (N=12).
Note: (A) HE staining images of histopathological changes in the kidneys of mice in each group (200×, scale bar = 50 μm); (B) Masson's trichrome staining images (400×, scale bar = 25 μm) and the corresponding quantitative analysis bar chart showing the fibrotic status in renal tissues of mice from each group. ***P<0.001.

In contrast, the high-dose quercetin alone group showed inhibitions of about 50% and 60%, while the S27673-MA alone group showed inhibitions of approximately 55% and 65%. The trends at the protein level were consistent with this (Fig. 4F). These findings indicate that quercetin and the PI3K pathway inhibitor have a synergistic anti-fibrotic effect, strongly suggesting that quercetin exerts its protective role by inhibiting the PI3K/Akt pathway and its downstream signaling.

DISCUSSION

This study demonstrates that quercetin effectively ameliorates aconitine-induced RIF through inhibition of the PI3K/Akt/NF-κB signaling axis. The findings not only expand the understanding of the mechanisms underlying aconitine nephrotoxicity but also provide new experimental evidence supporting quercetin as a potential therapeutic agent for intervening in drug-induced renal fibrosis. This study is the first to demonstrate the dose-dependent protective effect of quercetin in an aconitine-induced RIF model, with its core mechanism involving the suppression of abnormal PI3K/Akt pathway activation. This finding aligns with strategies targeting this pathway in fibrosis research across various organs. For instance, in cardiac fibrosis, xanthohumol alleviates lesions by modulating the PTEN/Akt/mTOR pathway (Sun *et al*., 2021) in pulmonary fibrosis and keloid formation, inhibition of PI3K/Akt signaling has also been confirmed as crucial (Jiang *et al*., 2024). These studies collectively establish Akt signaling as a "common pathway" in fibrosis. However, the innovation of this research lies in clarifying that, within the specific context of drug-induced kidney injury, this pathway functions by driving the NE/NF-κB axis, which couples inflammation and matrix degradation.

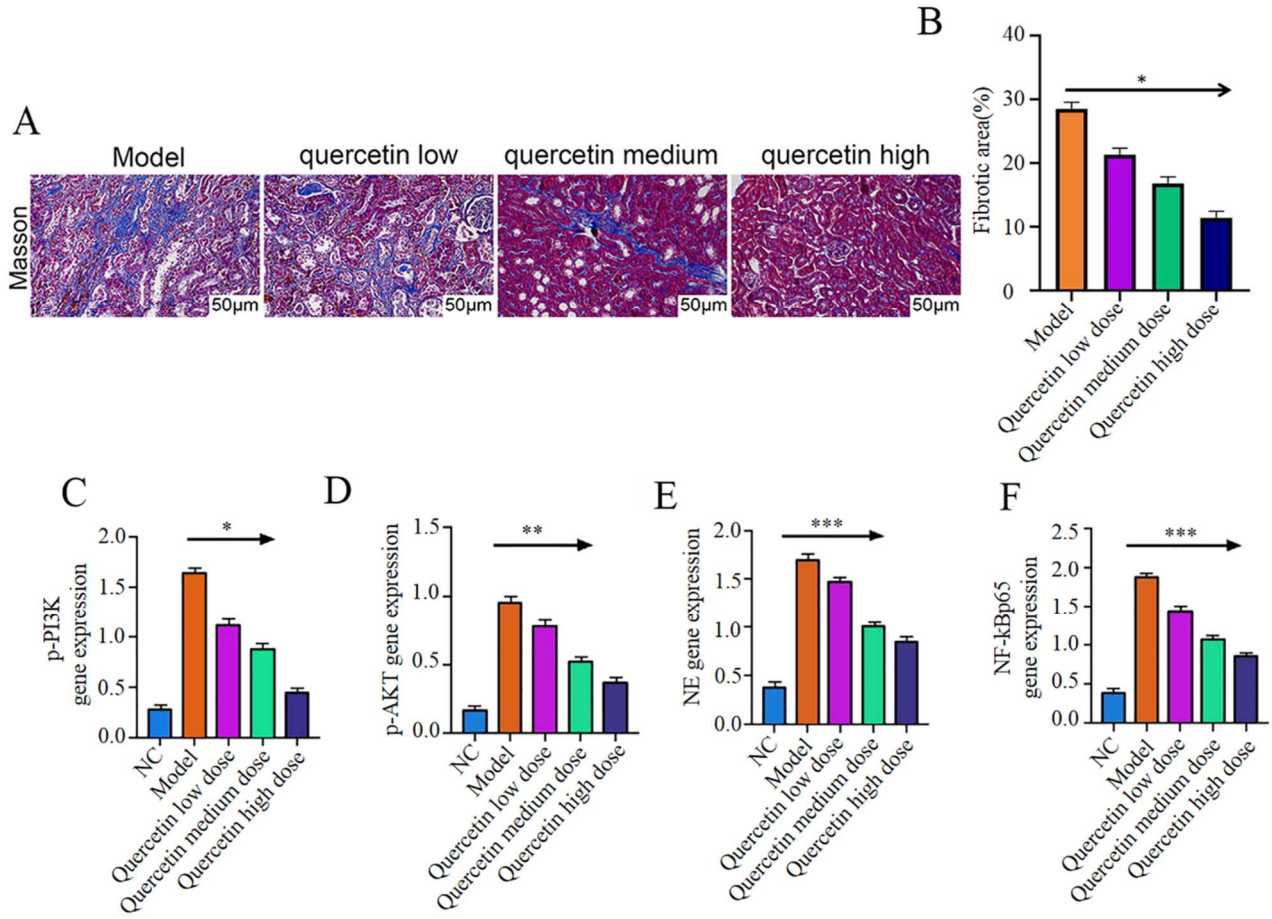

Fig. 2: Quercetin can affect RIF induced by aconitine (N=12).
Note: (A) HE staining of RIF in mice in each group (100×, scale bar = 100 μm); (B) Bar charts for quantitative analysis of renal tissue fibrosis status in each group of mice; (C) p-PI3K gene expression level (relative to control) in mice in each group; (D) p-AKT gene level (relative to control) in mice in each group ; (E) NE gene expression level (relative to control) of mice in each group; (F) NF-kBp65 gene expression level (relative to control) of mice in each group. **P*<0.05, ***P*<0.01, ****P*<0.001.

Table 2: Comparison of the number of CD+68 cells and F4/80+ cells in the renal interstitium of mice in each group (x±S).

Group	n	CD^{+}_{68} cell number (%)	$F4/80^{+}$ cell number (%)
NC group	12	6.25±1.16	4.98±1.06
Model group	12	18.68±2.34*	15.32±2.14*
Quercetin low dose group	12	12.32±1.62**	11.97±1.59**
Quercetin medium dose group	12	10.09±1.33**	9.65±1.23**
Quercetin high dose group	12	7.65±1.17**	6.87±1.05**
F value	-	34.086	45.635
P value	-	<0.001	<0.001

Note: Compared with NC group, *P<0.05; compared with model group, **P<0.05

Unlike the report, which indicated quercetin's protective role in diabetic encephalopathy through inhibition of ferroptosis (Cheng *et al*. 2024), this study reveals that quercetin's action in the kidney primarily focuses on regulating the inflammation-fibrosis transition, highlighting its multi-target and context-dependent characteristics across different pathophysiological environments.

The results of this study demonstrate that in the aconitine model group, the expression of p-PI3K, p-AKT and their downstream effectors NE and NF-κB p65 were synchronously upregulated. This suggests that the fibrogenic effect of aconitine is not solely due to direct cytotoxicity but rather initiates an inflammatory response-driven, cascade-amplifying signaling network.

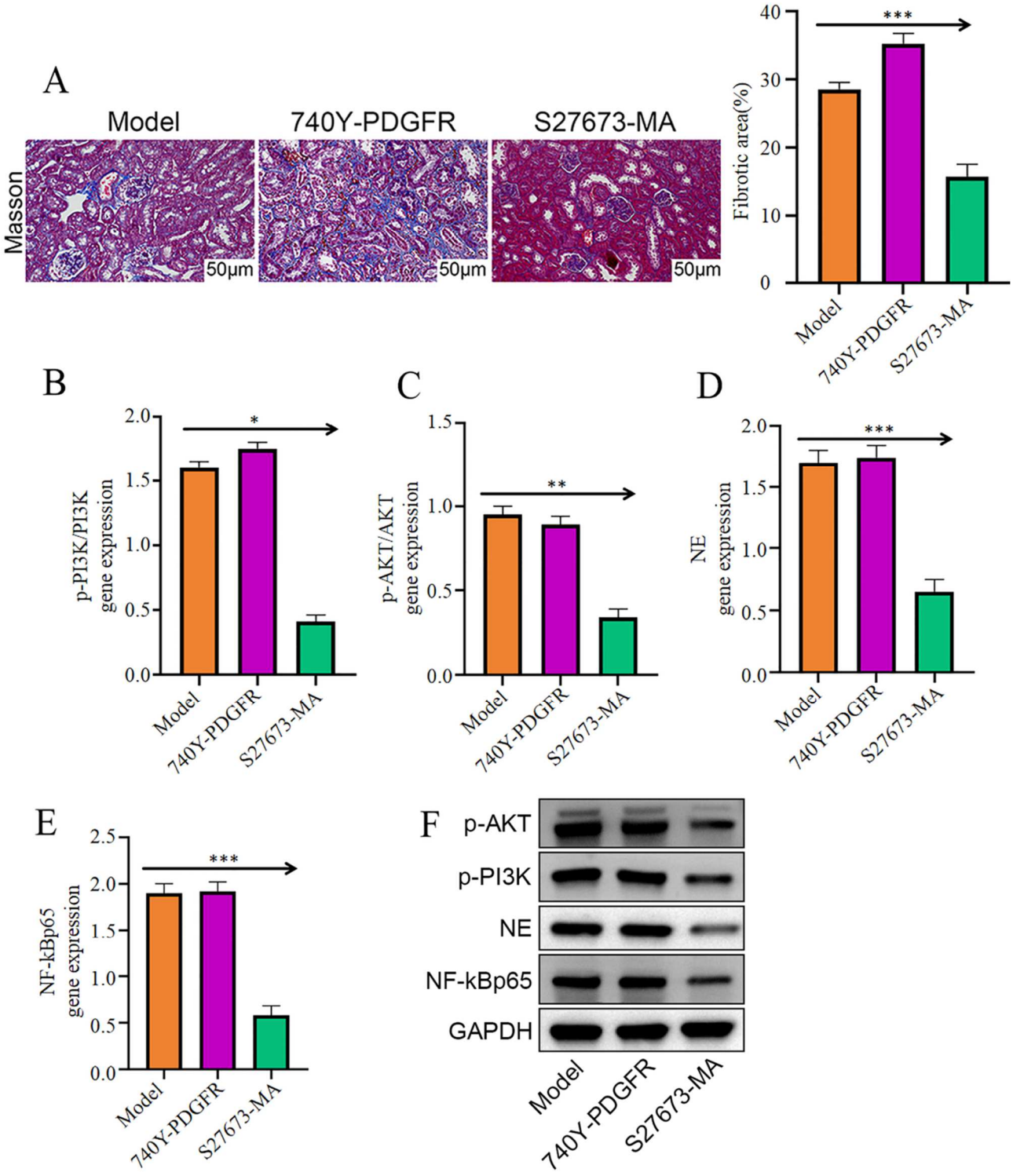

Fig. 3: PI3K/Akt pathway on RIF (N=12).

Note: (A) Masson staining images (400×, scale bar = 25 μm) of renal tissue fibrosis status in each group of mice and quantitative analysis bar charts; (B) p-PI3K gene expression level (relative to control) in mice in each group; (C) p-AKT gene level (relative to control) in mice in each group ; (D) NE gene expression level (relative to control) of mice in each group; (E) NF-kBp65 gene expression level (relative to control) of mice in each group; (F) WB pathway protein expression (relative to control) of mice in each group.*P<0.05, **P<0.01, ***P<0.001.

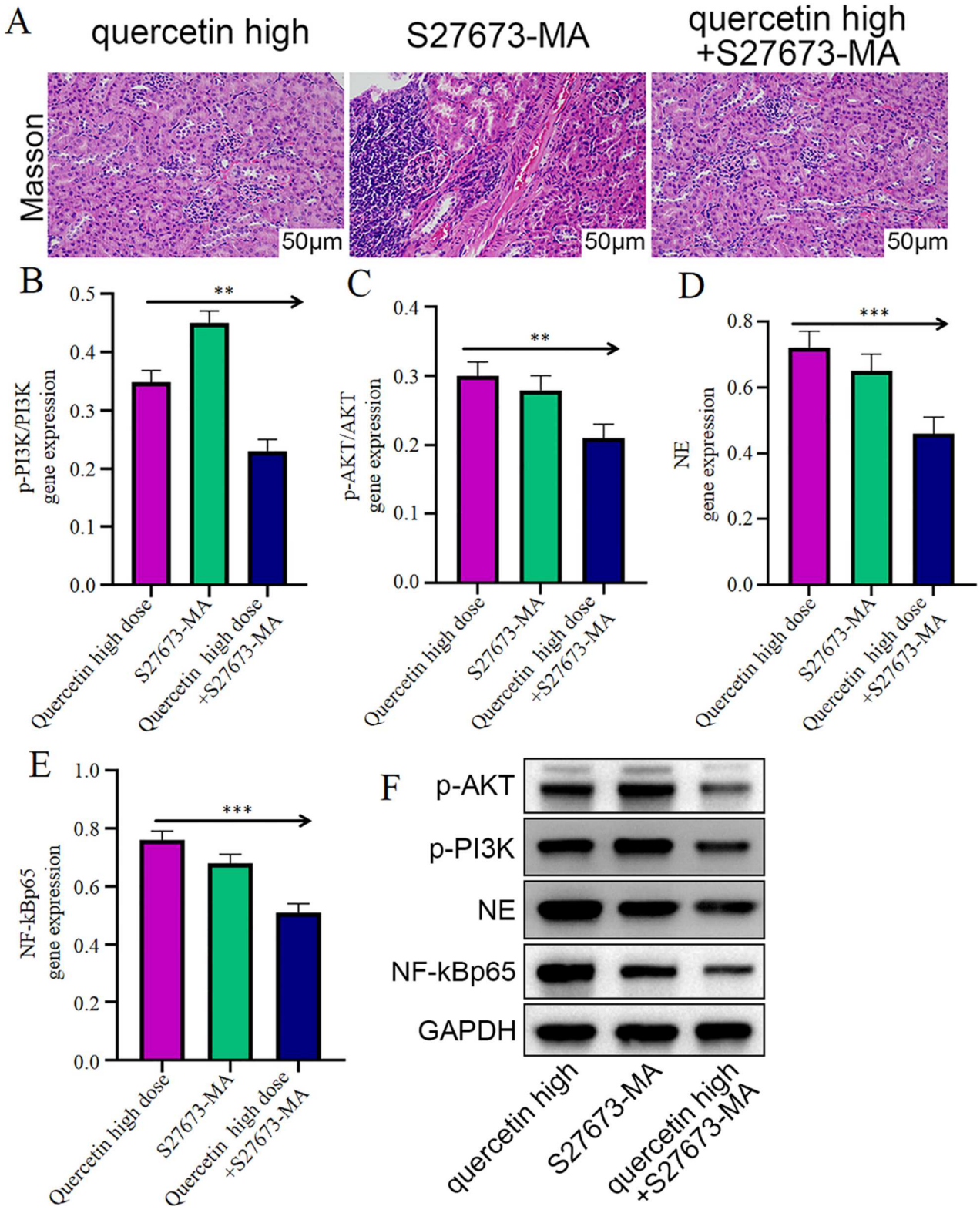

Fig. 4: Quercetin alleviates aconitine-induced RIF through the PI3K/Akt pathway (N=12).
Note: (A) HE staining of RIF in mice in each group (100×, scale bar = 100 μm); (B) p-PI3K gene expression level (relative to control) of mice in each group; (C) p-AKT gene expression level (relative to control) of mice in each group; (D) NE gene expression levels (relative to control) of mice in each group; (E) NF-kBp65 gene expression levels (relative to control) of mice in each group; (F) WB pathway protein expression (relative to control) of mice in each group.

Although the direct oxidative stress induced by aconitine may initially activate PI3K/Akt, subsequent inflammatory cell infiltration (such as increased $CD68^+$ and $F4/80^+$ macrophages) and the release of inflammatory mediators likely constitute the main driving forces for the sustained activation of this pathway and the progression of chronic fibrosis. This differs from certain growth factor-driven direct activation models and underscores the central role of the inflammation-to-fibrosis transition in drug-induced kidney injury. Moreover, the infiltrating macrophages ($CD68^+$, $F4/80^+$) appear to act as amplifiers in this process. Similarly, in viral myocarditis, exosomes derived from M2 macrophages regulate inflammatory outcomes by influencing metabolic reprogramming via the PKM2/HIF-1α axis (Zhang *et al*., 2024). This implies that in different organs, the metabolic and functional states of immune cells may be critical contextual factors determining the downstream effects of pathways like PI3K/Akt. Therefore, it is likely that aconitine induces the sustained activation of PI3K/Akt through a combination of direct damage and indirect immune-inflammatory responses.

The molecular changes such as —p-PI3K, p-AKT, NE and NF-κB—collectively depict a pathological progression from early injury signals (PI3K/Akt activation) to inflammatory amplification (NF-κB upregulation) and, ultimately, tissue destruction and matrix remodeling. Notably, NE (neutrophil elastase) is not only an inflammatory marker but also directly degrades extracellular matrix components and activates latent pro-fibrotic factors, serving as a key effector molecule linking inflammation and fibrotic collapse. Its upregulation signifies the entry into an active phase of tissue destruction (Cai *et al*., 2024, Narasaraju *et al*., 2024). This suggests that monitoring such molecular changes may help identify patients at high risk for fibrosis progression. Recent research on Geraniin's anti-cancer effects in breast cancer models through the regulation of specific plasma proteins is also exploring the use of dynamic changes in the plasma proteome to assess disease progression and treatment response (Yu *et al*., 2026). Although this study is based on an animal model, the sustained activation of the PI3K/Akt–NF-κB–NE molecular axis likely corresponds to the critical stage in clinical chronic kidney disease where inflammatory responses following acute kidney injury transition into irreversible interstitial fibrosis. This provides clues for the future identification of clinical biomarkers to intervene in this specific pathological phase.

The protective effect of quercetin stems from both its antioxidant capacity and its targeted modulation of signaling pathways. On the one hand, its classic antioxidant activity helps scavenge ROS generated by aconitine, thereby mitigating the activation of pathways such as PI3K/Akt from the source (Biswas *et al*., 2022). On the other hand, this study found that quercetin directly and dose-dependently downregulates the phosphorylation of p-PI3K and p-AKT. This precise modulation of specific kinase signaling reflects the "drug-like" characteristics of natural compounds that go beyond basic antioxidant functions. The synergistic effect observed in the combination experiment strongly demonstrates that inhibiting this pathway is one of the primary mechanisms underlying its anti-fibrotic action, further robustly proving that pharmacological inhibition of this pathway is a key mechanism through which quercetin exerts its anti-fibrotic effects, rather than merely being a byproduct of its antioxidant activity. This aligns with the approach of Wang *et al*. (2025), who optimized the activity of quinoline derivatives through chemical modification strategies such as C3-H trifluoroacetylation, emphasizing that precise regulation of the core pharmacophore is crucial for achieving desired therapeutic efficacy. Furthermore, recent studies have revealed novel mechanisms of quercetin in other disease models, such as protecting nerve cells by activating Nrf2 or directly inhibiting ferroptosis (Cheng *et al*., 2024). Although ferroptosis markers were not examined in this model, it cannot be ruled out that aconitine nephrotoxicity is partly driven by lipid peroxidation, which quercetin may simultaneously intervene in. Additionally, research by Zhang *et al*. (2024) on macrophage metabolic reprogramming suggests that quercetin may also alter the pro-fibrotic phenotype of renal immune cells by influencing their energy metabolism, potentially representing another regulatory pathway independent of the classic PI3K/Akt axis. Thus, while the primary and direct mechanism through which quercetin ameliorates aconitine-induced RIF is the inhibition of the PI3K/Akt pathway and its downstream NF-κB/NE axis—strongly supported by gain- and loss-of-function experiments—its inherent antioxidant properties and potential modulation of other cell death programs or cellular metabolism constitute important synergistic or background protective networks. This multi-target characteristic is precisely the advantage of many natural products. However, it also highlights the need for more refined future studies to dissect the relative contributions of each pathway.

The doses of quercetin selected for this experiment (50, 100, 150 mg/kg) were based on literature reporting efficacy in rodent models of renal fibrosis (Liu *et al*., 2019). Although these doses are higher than the typical daily intake of dietary flavonoids in humans, they are reasonable for pharmacological studies in animals. Given quercetin's relatively limited bioavailability *in-vivo*, this dosage range was chosen to achieve an effective concentration in the target organ sufficient to produce a clear pharmacological effect. Future translational research should focus on the development of novel drug delivery systems for quercetin to enhance its bioavailability, thereby reducing the

effective dose and improving the feasibility of clinical application.

This study, through *in-vivo* experiments and molecular mechanism investigations, confirms that quercetin alleviates aconitine-induced renal interstitial fibrosis by targeting and inhibiting the PI3K/Akt signaling pathway and its downstream NE/NF-κB axis. This provides important preclinical evidence for developing quercetin as a therapeutic agent for preventing and treating drug-induced kidney injury and subsequent fibrosis.

Nevertheless, several limitations of this study should be acknowledged: First, the aconitine dosing regimen (1.0 mg/kg) was designed to establish a stable fibrosis model, but the accompanying acute toxic symptoms (e.g., neurotoxicity) may confound some observations. Second, while fibrosis was assessed quantitatively through histological staining, direct quantitative detection of classic fibrosis markers such as Collagen I/III or α-SMA at the protein level was lacking. Third, the study did not include renal function indicators such as serum creatinine, blood urea nitrogen, or urinary protein, leaving the direct correlation between pathological improvement and functional recovery not fully elucidated. Fourth, the Western blot results are presented as data graphs without representative blot images, which affects the intuitive presentation of the results.

Future research should address these limitations by: (1) Establishing chronic renal fibrosis models with lower toxicity and higher specificity. (2) Quantitatively detecting α-SMA, Col I/III and utilizing immunofluorescence for cellular localization. (3) Incorporating SCr, BUN, UPCR and injury markers for correlation analysis. (4) Supplementing complete raw data images and further pursuing translational studies focusing on dose optimization, delivery systems and genetic validation.

CONCLUSION

In conclusion, quercetin significantly alleviated aconitine-induced renal interstitial fibrosis, collagen deposition and inflammatory infiltration in mice, likely through dose-dependent inhibition of the PI3K/Akt pathway and its downstream NF-κB/NE axis. This provides important experimental evidence supporting quercetin as a potential candidate for preventing and treating drug-induced renal fibrosis. Although this study elucidated its protective effects from pathological and molecular perspectives, the lack of renal function indicators and direct evidence regarding classic fibrotic proteins such as α-SMA means its precise clinical relevance still requires further confirmation. Future research involving optimized models, validation of functional improvement and enhanced bioavailability is warranted.

Acknowledgments
None.

Authors' contribution
Wei Feng and Jie Zhou: Responsible for experimental design and overall planning, establishment and grouping of the experimental animal model, data organization and statistical analysis, drafting and revising the initial manuscript and final review and approval of the article; Yuanjue Zheng: Responsible for performing specific animal experimental procedures (including drug administration and specimen collection), preparation and staining of histopathological sections (HE and Masson staining) and acquisition and preliminary organization of experimental data; Yingang Li: Responsible for conducting molecular biology experiments (including qPCR and Western blot) and analyzing the data, procurement and management of experimental reagents, acquisition and management of research funding, manuscript revision and review and fulfilling the role of corresponding author (including manuscript submission and communication with the journal).

Funding
There was no funding.

Data availability statement
The datasets generated and/or analyzed during the current study are available from the corresponding author on reasonable request.

Ethical approval
This study was approved by the ethics committee of The First Affiliated Hospital of Zhengzhou University (Approval No.: GLP20250928). All experimental animal procedures followed the "3R" principles to minimize animal suffering. This study was performed in adherence with the ARRIVE guidelines. See supplementary file for the ARRIVE checklist.

Conflict of interest
The authors state that this research was conducted without any commercial or financial interests that could be interpreted as potential conflicts of interest.

Supplementary data
https://www.pjps.pk/uploads/2026/06/SUP1781939289.pdf

REFERENCES

Biswas P, Dey D, Biswas PK, Rahaman TI, Saha S, Parvez A, Khan DA, Lily NJ, Saha K, Sohel M, Hasan MM, Al Azad S, Bibi S, Hasan MN, Rahmatullah M, Chun J, Rahman MA and Kim B (2022). A comprehensive analysis and anti-cancer activities of quercetin in ROS-

mediated cancer and cancer stem cells. *Int J Mol Sci*., **23**(19): 11746.

Cai M, Deng J, Wu S, Cao Y, Chen H, Tang H, Zou C, Zhu H and Qi L (2024). Alpha-1 antitrypsin targeted neutrophil elastase protects against sepsis-induced inflammation and coagulation in mice via inhibiting neutrophil extracellular trap formation. *Life Sci*., **353**: 122923.

Cheng X, Huang J, Li H, Zhao D, Liu Z, Zhu L, Zhang Z and Peng W (2024). Quercetin: A promising therapy for diabetic encephalopathy through inhibition of hippocampal ferroptosis. *Phytomedicine*., **126**: 154887.

Hao X, Jin Y, Zhang Y, Li S, Cui J, He H, Guo L, Yang F and Liu H (2023). Inhibition of oncogenic src ameliorates silica-induced pulmonary fibrosis via PI3K/AKT pathway. *Int J Mol Sci*., **24**(1): 774.

He H, Sun S, Zhang M and Shou L (2025). Research on erchen tang in the treatment of community-acquired pneumonia based on chemical molecular mechanisms of quercetin and kaempferol: PI3K/AKT/NF-κB protein signaling. *Int J Biol Macromol*., **311**(Pt 4): 144071.

Hu T, Chen F, Chen D and Liang H (2022). DNMT3a negatively regulates PTEN to activate the PI3K/AKT pathway to aggravate renal fibrosis. *Cell Signal*., **96**: 110352.

Jiang Z, Chen Z, Xu Y, Li H, Li Y, Peng L, Shan H, Liu X, Wu H, Wu L, Jian D, Su J, Chen X, Chen Z and Zhao S (2024). Low-frequency ultrasound sensitive piezo1 channels regulate keloid-related characteristics of fibroblasts. *Adv Sci (Weinh)*., **11**(14): e2305489.

Liu T, Yang Q, Zhang X, Qin R, Shan W, Zhang H and Chen X (2020). Quercetin alleviates kidney fibrosis by reducing renal tubular epithelial cell senescence through the SIRT1/PINK1/mitophagy axis. *Life sciences*, **257**: 118116.

Liu Y, Dai E and Yang J (2019). Quercetin suppresses glomerulosclerosis and TGF-β signaling in a rat model. *Mol Med Rep*., **19**(6): 4589–4596.

Narasaraju T, Neeli I, Criswell SL, Krishnappa A, Meng W, Silva V, Bila G, Vovk V, Serhiy Z, Bowlin GL, Meyer N, Luning Prak ET, Radic M and Bilyy R (2024). Neutrophil activity and extracellular matrix degradation: Drivers of lung tissue destruction in fatal COVID-19 cases and implications for long COVID. *Biomolecules*., **14**(2): 236.

Rui Y, Zhang X, Min X, Xie H, Ma X, Geng F and Liu R (2024). Unlocking renal restoration: Mesaconine from aconitum plants restore mitochondrial function to halt cell apoptosis in acute kidney injury. *Int Immunopharmacol*., **133**: 112170.

Sun TL, Li WQ, Tong XL, Liu XY and Zhou WH (2021). Xanthohumol attenuates isoprenaline-induced cardiac hypertrophy and fibrosis through regulating PTEN/AKT/mTOR pathway. *Eur J Pharmacol*., **891**: 173690.

Wang X, Yan A, Xiao H, Xiao W, Xu L and Wang D (2025). C3-H trifluoroacetylation of quinolines and pyridines: Access to heteroaryl ketones, carboxylic acids and amides. *Org Lett*., **27**(22): 5625–5631.

Wang Y, Han Y, Shang K, Xiao J, Tao L, Peng Z, Liu S and Jiang Y (2024). Kokusaginine attenuates renal fibrosis by inhibiting the PI3K/AKT signaling pathway. *Biomed Pharmacother*., **175**: 116695.

Xiang G, Xing N, Wang S and Zhang Y (2023). Antitumor effects and potential mechanisms of aconitine based on preclinical studies: An updated systematic review and meta-analysis. *Front Pharmacol*., **14**: 1172939.

Xu A, Deng F, Chen Y, Kong Y, Pan L, Liao Q, Rao Z, Xie L, Yao C, Li S, Zeng X, Zhu X, Liu H, Gao N, Xue L, Chen F, Xu G, Wei D, Zhou X, Li Z and Sheng X (2020). NF-κB pathway activation during endothelial-to-mesenchymal transition in a rat model of doxorubicin-induced cardiotoxicity. *Biomed Pharmacother*., **130**: 110525.

Yu J, Li Y, Li Y, Liu X, Huo Q, Wu N, Zhang Y, Zeng T, Zhang Y, Li HY, Lian J, Zhou J, Moses EJ, Geng J, Lin J, Li W and Zhu X (2025). Phosphorylation of FOXN3 by NEK6 promotes pulmonary fibrosis through Smad signaling. *Nature communications*, **16**(1): 1865.

Yangzom P, Amruthanand S, Sharma M, Mahajan S, Lingaraju MC, Parida S, Sahoo M, Kumar D and Singh TU (2022). Subacute 28 days oral toxicity study of kaempferol and biochanin-A in the mouse model. *J Biochem Mol Toxicol*., **36**(8): e23090.

Yu Y, Ye X, Hou T, Zhou H, Liu L, Yuan W, Wang J and Liang X (2026). A natural LDHA allosteric inhibitor geraniin suppresses triple-negative breast cancer cell growth. *Phytother Res*., **40**(1): 21–34.

Zhang J, Guo J, Qian Y, Yu L, Ma J, Gu B, Tang W, Li Y, Li H and Wu W (2025). Quercetin induces apoptosis through downregulating P4HA2 and inhibiting the PI3K/Akt/mTOR axis in hepatocellular carcinoma cells: An *in-vitro* study. *Cancer Rep (Hoboken)*., **8**(5): e70220.

Zeng YF, Li JY, Wei XY, Ma SQ, Wang QG, Qi Z, Duan ZC, Tan L and Tang H (2023). Preclinical evidence of reno-protective effect of quercetin on acute kidney injury: A meta-analysis of animal studies. *Frontiers in pharmacology*, **14**: 1310023.

Zhang Y, Zhu L, Li X, Ge C, Pei W, Zhang M, Zhong M, Zhu X and Lv K (2024). M2 macrophage exosome-derived lncRNA AK083884 protects mice from CVB3-induced viral myocarditis through regulating PKM2/HIF-1α axis mediated metabolic reprogramming of macrophages. *Redox Biol*., **69**: 103016.

Zhang Y, Zhu L, Li X, Ge C, Pei W, Zhang M, Zhong M, Zhu X and Lv K (2024). M2 macrophage exosome-derived lncRNA AK083884 protects mice from CVB3-induced viral myocarditis through regulating PKM2/HIF-1α axis mediated metabolic reprogramming of macrophages. *Redox Biol*., **69**: 103016.